

Statefinder Diagnostic and $w - w'$ Analysis for the Agegraphic Dark Energy Models without and with Interaction

Hao Wei^{1,*} and Rong-Gen Cai^{2,†}

¹*Department of Physics and Tsinghua Center for Astrophysics,
Tsinghua University, Beijing 100084, China*

²*Institute of Theoretical Physics, Chinese Academy of Sciences,
P.O. Box 2735, Beijing 100080, China*

Abstract

A new dark energy model, named as “agegraphic dark energy”, has been proposed by one of us (R. G. Cai) in arXiv:0707.4049, based on the Károlyházy uncertainty relation, which arises from the quantum mechanics together with general relativity. Then, in arXiv:0707.4052, it has been extended by including the interaction between the agegraphic dark energy and the pressureless (dark) matter. In this note, we investigate the agegraphic dark energy models without and with interaction by means of statefinder diagnostic and $w - w'$ analysis.

PACS numbers: 95.36.+x, 98.80.Qc, 98.80.-k

* email address: haowei@mail.tsinghua.edu.cn

† email address: cairg@itp.ac.cn

The cosmological constant problem is essentially a problem in quantum gravity, since the cosmological constant is commonly considered as the vacuum expectation value of some quantum fields. Before a completely successful quantum theory of gravity is available, it is more realistic to combine the quantum mechanics with general relativity directly.

In general relativity, one can measure the spacetime without any limit of accuracy. However, in quantum mechanics, the well-known Heisenberg uncertainty relation puts a limit of accuracy in these measurements. Following the line of quantum fluctuations of spacetime, Károlyházy and his collaborators [1] (see also [2]) made an interesting observation concerning the distance measurement for Minkowski spacetime through a light-clock *Gedanken experiment*, namely, the distance t in Minkowski spacetime cannot be known to a better accuracy than

$$\delta t = \lambda t_p^{2/3} t^{1/3}, \quad (1)$$

where λ is a dimensionless constant of order unity. We use the units $\hbar = c = k_B = 1$ throughout this work. Thus, one can use the terms like length and time interchangeably, whereas $l_p = t_p = 1/m_p$ with l_p , t_p and m_p being the reduced Planck length, time and mass respectively.

The Károlyházy relation (1) together with the time-energy uncertainty relation enables one to estimate a quantum energy density of the metric fluctuations of Minkowski spacetime [3, 2]. Following [3, 2], with respect to the Eq. (1) a length scale t can be known with a maximum precision δt determining thereby a minimal detectable cell $\delta t^3 \sim t_p^2 t$ over a spatial region t^3 . Such a cell represents a minimal detectable unit of spacetime over a given length scale t . If the age of the Minkowski spacetime is t , then over a spatial region with linear size t (determining the maximal observable patch) there exists a minimal cell δt^3 the energy of which due to time-energy uncertainty relation can not be smaller than [3, 2]

$$E_{\delta t^3} \sim t^{-1}. \quad (2)$$

Therefore, the energy density of metric fluctuations of Minkowski spacetime is given by [3, 2]

$$\rho_q \sim \frac{E_{\delta t^3}}{\delta t^3} \sim \frac{1}{t_p^2 t^2} \sim \frac{m_p^2}{t^2}. \quad (3)$$

We refer to the original papers [3, 2] for more details. It is worth noting that in fact, the Károlyházy relation (1) and the corresponding energy density (3) have been independently rediscovered later for many times in the literature (see e.g. [39, 40, 41]).

In [4], one of us (R.G.C.) proposed a new dark energy model based on the energy density Eq. (3). As the most natural choice, the length measure t in Eq. (3) is chosen to be the age of the universe

$$T = \int_0^a \frac{da}{Ha}, \quad (4)$$

where a is the scale factor of our universe; $H \equiv \dot{a}/a$ is the Hubble parameter; a dot denotes the derivative with respect to cosmic time. Therefore, we call it as ‘‘agegraphic dark energy’’. The energy density of the agegraphic dark energy is given by [4]

$$\rho_q = \frac{3n^2 m_p^2}{T^2}, \quad (5)$$

where the numerical factor $3n^2$ is introduced to parameterize some uncertainties, such as the species of quantum fields in the universe, the effect of curved spacetime, and so on. Since the energy density (3) is derived for Minkowski spacetime, the factor $3n^2$ also compiles the effects coming from the straightforward

application of Eq. (3) in the Friedmann-Robertson-Walker (FRW) spacetime. Obviously, since the present age of the universe $T_0 \sim H_0^{-1}$ (the subscript “0” indicates the present value of the corresponding quantity; we set $a_0 = 1$), the present energy density of the agegraphic dark energy explicitly meets the observed value naturally, provided that the numerical factor n is of order unity. It is shown that the agegraphic dark energy naturally obeys the holographic black hole entropy bound [3, 4], just like the holographic dark energy. In addition, by choosing the age of the universe rather than the future event horizon as the length measure, the drawback concerning causality in the holographic dark energy model [5] (see also e.g. [6, 7] for relevant references) does not exist in the agegraphic dark energy model [4]. The similarity and difference between the agegraphic dark energy and holographic dark energy are discussed in [8].

We consider a flat Friedmann-Robertson-Walker (FRW) universe containing agegraphic dark energy and pressureless matter, the corresponding Friedmann equation reads

$$H^2 = \frac{1}{3m_p^2} (\rho_m + \rho_q). \quad (6)$$

It is convenient to introduce the fractional energy densities $\Omega_i \equiv \rho_i/(3m_p^2 H^2)$ for $i = m$ and q . From Eq. (5), it is easy to find that

$$\Omega_q = \frac{n^2}{H^2 T^2}, \quad (7)$$

whereas $\Omega_m = 1 - \Omega_q$ from Eq. (6). By using Eqs. (5), (7) and the energy conservation equation $\dot{\rho}_m + 3H\rho_m = 0$, we obtain the equation of motion for Ω_q as [4]

$$\Omega'_q = \Omega_q (1 - \Omega_q) \left(3 - \frac{2}{n} \sqrt{\Omega_q} \right), \quad (8)$$

where a prime denotes the derivative with respect to the e -folding time $N \equiv \ln a$. From the energy conservation equation $\dot{\rho}_q + 3H(\rho_q + p_q) = 0$, Eqs. (5) and (7), it is easy to find that the equation-of-state parameter (EoS) of the agegraphic dark energy $w_q \equiv p_q/\rho_q$ is given by [4]

$$w_q = -1 + \frac{2}{3n} \sqrt{\Omega_q}. \quad (9)$$

In addition, differentiating Eqs. (6) and using Eqs. (5), (7), and the energy conservation equation $\dot{\rho}_m + 3H\rho_m = 0$, we obtain the deceleration parameter as [8]

$$q \equiv -\frac{\ddot{a}}{aH^2} = -1 - \frac{\dot{H}}{H^2} = \frac{1}{2} - \frac{3}{2}\Omega_q + \frac{\Omega_q^{3/2}}{n}. \quad (10)$$

Notice that the scale factor $a(t)$ can be explicitly expanded as

$$a(t) = a_0 \left[1 + H_0(t - t_0) - \frac{1}{2}q_0 H_0^2 (t - t_0)^2 + \frac{1}{6} \frac{\ddot{a}}{a} \Big|_{t_0} (t - t_0)^3 + \dots \right]$$

around the present time $t = t_0$. Naturally, the next step beyond $H \equiv \dot{a}/a$ and $q \equiv -\ddot{a}/(aH^2)$ is to consider a new geometrical quantity containing \ddot{a} . In fact, a so-called statefinder pair $\{r, s\}$ has been introduced in [9], namely

$$r \equiv \frac{\ddot{a}}{aH^3}, \quad s \equiv \frac{r - 1}{3(q - 1/2)}, \quad (11)$$

where s is a combination of r and q . So, the coefficient of the third term in the Taylor's expansion of $a(t)$ can be conveniently expressed as $r_0 H_0^3/6$. It is obvious that the statefinder is a geometrical diagnostic

because it depends only on the scale factor a . The well-known Λ CDM model corresponds to a fixed point $\{r = 1, s = 0\}$ in the $r - s$ diagram [9]. Since different cosmological models exhibit qualitatively different trajectories of evolution in the $r - s$ plane, the statefinder is a good tool to distinguish cosmological models [9]. In fact, the statefinder diagnostic has been extensively used in many models, such as Λ CDM, quintessence [9, 10], Chaplygin gas [11, 10], DGP braneworld [9, 10], interacting quintessence model [12, 13], the holographic dark energy models without and with interaction [14, 15], the holographic dark energy model in non-flat universe [16], quintom [17], interacting phantom model [18], five-dimensional cosmology [19], Cardassian model [20], bulk viscous cosmology [21], tachyon [22], and so on. As shown in [10, 23], the statefinder diagnostic combined with the future SNAP observation can be used to discriminate different cosmological models.

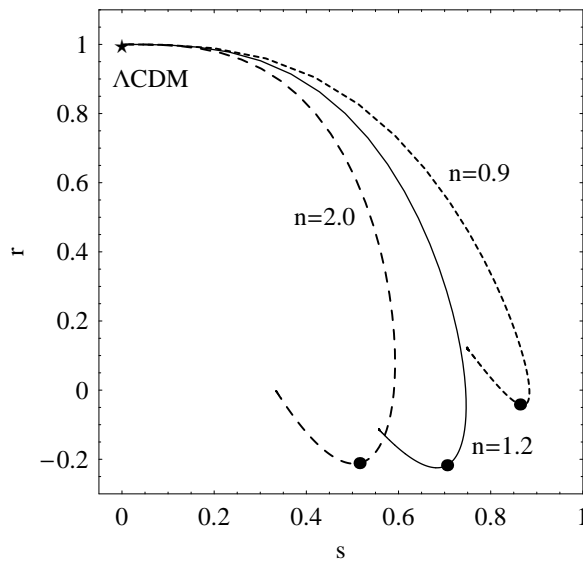


Figure 1: Evolution trajectories of the statefinder in the $r - s$ plane for different model parameter n in the agegraphic dark energy model without interaction. The solid points indicate the present values of the statefinder. The statefinder for the Λ CDM model is a fixed point and is also indicated by a star symbol.

In this note, we study the agegraphic dark energy by means of the statefinder diagnostic. By using the Friedmann equation, i.e. Eq. (6), and the Raychaudhuri equation

$$\dot{H} = -\frac{1}{2m_p^2} (\rho_m + \rho_q + p_q), \quad (12)$$

from the definitions Eq. (11), one can find that [9, 10]

$$r = 1 + \frac{9}{2}\Omega_q w_q (1 + w_q) - \frac{3}{2}\Omega_q w'_q, \quad (13)$$

$$s = 1 + w_q - \frac{w'_q}{3w_q}. \quad (14)$$

Differentiating Eq. (9) and using Eq. (8), we get

$$w'_q = \frac{\sqrt{\Omega_q}}{3n} (1 - \Omega_q) \left(3 - \frac{2}{n} \sqrt{\Omega_q} \right). \quad (15)$$

One can solve Eq. (8) to get the $\Omega_q(z)$, where z is the redshift. Note that in the numerical integration of Eq. (8) we use the initial condition $\Omega_{q0} = 0.73$. Substituting into Eqs. (15), (13) and (14), the statefinder $\{r(z), s(z)\}$ is in hand. In Fig. 1, we show the evolution trajectories of the statefinder in the $r - s$ plane for different model parameter n in the agegraphic dark energy model without interaction. While the universe expands, the trajectories of the statefinder start from the point $\{r = 1, s = 0\}$ at $z \rightarrow \infty$ (i.e. $a \rightarrow 0$), then s increases to a maximum and r decreases to a minimum, after that the trajectories turn a corner and approach another final fixed points at $z \rightarrow -1$ (i.e. $a \rightarrow \infty$). In fact, from Eqs. (9) and (15), it is easy to see that $w_q \rightarrow -1$ and $w'_q \rightarrow 0$ while $\Omega_q \rightarrow 0$ when $a \rightarrow 0$, thus $r \rightarrow 1$ and $s \rightarrow 0$ from Eqs. (13) and (14). The agegraphic dark energy mimics the cosmological constant in the early stage. Similarly, one can also find out the final fixed point in the $r - s$ plane. From Eqs. (9) and (15), we find that $w_q \rightarrow -1 + 2/(3n)$ and $w'_q \rightarrow 0$ while $\Omega_q \rightarrow 1$ when $a \rightarrow \infty$, therefore $r \rightarrow 1 + 2/n^2 - 3/n$ and $s \rightarrow 2/(3n)$ at that time. From Fig. 1, we see that the trajectories of the statefinder for different model parameter n can be significantly distinguished. The present value of s is smaller when n is larger. It is worth noting that the present values of the statefinder for the agegraphic dark energy model without interaction are fairly far from the one for the Λ CDM model, unless n is very large. Therefore, the statefinder diagnostic combined with the future SNAP observation can easily discriminate the agegraphic dark energy model without interaction from the Λ CDM model.

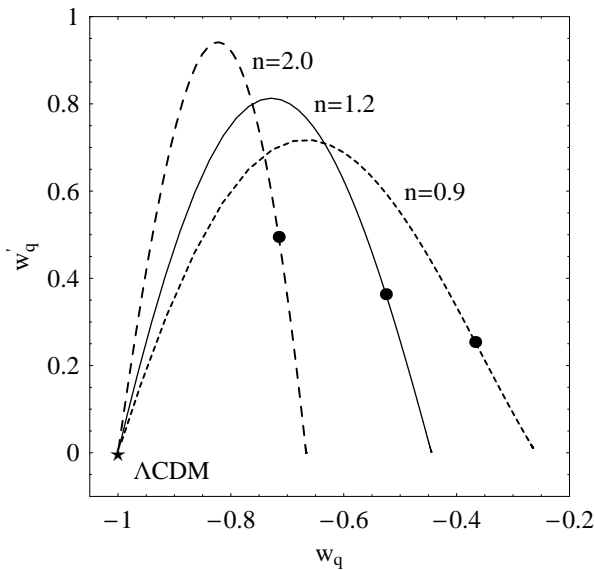


Figure 2: Evolution trajectories of $\{w_q, w'_q\}$ for different model parameter n in the agegraphic dark energy model without interaction. The solid points indicate the present values of $\{w_q, w'_q\}$. The $\{w, w'\}$ of the Λ CDM model is a fixed point and is also indicated by a star symbol.

In addition to the statefinder $r - s$ which is a geometrical diagnostic, there is other dynamical diagnostic $w - w'$ which is also used extensively in the literature. Similar to the scale factor, the

Taylor's expansion of the EoS reads $w(N) = w(N = N_0) + w'(N - N_0)/2 + \dots$ around $N = N_0$. So, the $w - w'$ analysis is important to discriminate models. The $w - w'$ analysis was first proposed in [24], and then was extended in [25, 26]. See e.g. [27, 28, 29, 30, 31, 32, 15, 16] for relevant works, and a recent review can be found in [33]. The well-known Λ CDM model corresponds to a fixed point $\{w = -1, w' = 0\}$ in the $w - w'$ plane. In the agegraphic dark energy model without interaction, the w_q and w'_q are given in Eqs. (9) and (15). Again, one can solve Eq. (8) to get the $\Omega_q(z)$, and then obtain the $w_q(z)$ and $w'_q(z)$. In Fig. 2, we show the evolution trajectories of $\{w_q, w'_q\}$ for different model parameter n in the agegraphic dark energy model without interaction. While the universe expands, the trajectories start from the point $\{w_q = -1, w'_q = 0\}$ at $z \rightarrow \infty$ (i.e. $a \rightarrow 0$), then w'_q increases to a maximum, after that the trajectories turn a corner and approach another final fixed points at $z \rightarrow -1$ (i.e. $a \rightarrow \infty$). As mentioned above, when $a \rightarrow 0$, the agegraphic dark energy mimics a cosmological constant. From Eqs. (9) and (15), one can find that $w_q \rightarrow -1 + 2/(3n)$ and $w'_q \rightarrow 0$ when $a \rightarrow \infty$. From Fig. 2, we see that the trajectories of $\{w_q, w'_q\}$ for different model parameter n can be significantly distinguished. The present w_q is smaller and the present w'_q is larger when n is larger. In addition, we can clearly see that w_q is always larger than -1 and cannot cross the phantom divide $w = -1$, cf. Eq. (9).

In [8], we have extended the original agegraphic dark energy model by including the interaction between the agegraphic dark energy and the pressureless (dark) matter. We assume that the agegraphic dark energy and pressureless (dark) matter exchange energy through interaction term Q , namely

$$\dot{\rho}_q + 3H(\rho_q + p_q) = -Q, \quad (16)$$

$$\dot{\rho}_m + 3H\rho_m = Q, \quad (17)$$

which preserves the total energy conservation equation $\dot{\rho}_{tot} + 3H(\rho_{tot} + p_{tot}) = 0$. From Eq. (7), we get

$$\Omega'_q = \Omega_q \left(-2\frac{\dot{H}}{H^2} - \frac{2}{n}\sqrt{\Omega_q} \right). \quad (18)$$

Differentiating Eq. (6) and using Eqs. (17), (5) and (7), it is easy to find that

$$-\frac{\dot{H}}{H^2} = \frac{3}{2}(1 - \Omega_q) + \frac{\Omega_q^{3/2}}{n} - \frac{Q}{6m_p^2 H^3}. \quad (19)$$

Therefore, we obtain the the equation of motion for Ω_q as

$$\Omega'_q = \Omega_q \left[(1 - \Omega_q) \left(3 - \frac{2}{n}\sqrt{\Omega_q} \right) - Q_1 \right]. \quad (20)$$

where

$$Q_1 \equiv \frac{Q}{3m_p^2 H^3}. \quad (21)$$

If $Q = 0$, Eq. (20) reduces to Eq. (8). From Eqs. (16), (5) and (7), we get the EoS of the agegraphic dark energy as

$$w_q = -1 + \frac{2}{3n}\sqrt{\Omega_q} - Q_2, \quad (22)$$

where

$$Q_2 \equiv \frac{Q}{3H\rho_q}. \quad (23)$$

Again, if $Q = 0$, Eq. (22) reduces to Eq. (9). By using the total EoS $w_{tot} \equiv p_{tot}/\rho_{tot} = -1 - \frac{2}{3}\frac{\dot{H}}{H^2} = -1/3 + 2q/3$ and $w_{tot} = \Omega_q w_q$, we find that

$$q = \frac{1}{2} + \frac{3}{2}\Omega_q w_q. \quad (24)$$

Here, it is also of interest to study the interacting agegraphic dark energy model by means of statefinder diagnostic and $w - w'$ analysis. From the definition Eq. (11), it is easy to find that

$$r = \frac{\ddot{H}}{H^3} - 3q - 2. \quad (25)$$

From Eqs. (12), (16) and (17), after some algebra, we have

$$\frac{\ddot{H}}{H^3} = \frac{9}{2} + \frac{9}{2}\Omega_q w_q (w_q + 2) - \frac{3}{2}\Omega_q w'_q + \frac{3}{2}Q_1 w_q. \quad (26)$$

Substituting Eqs. (24) and (26) into Eq. (25), we finally obtain that

$$r = 1 + \frac{9}{2}\Omega_q w_q (1 + w_q) - \frac{3}{2}\Omega_q w'_q + \frac{3}{2}Q_1 w_q. \quad (27)$$

From the definition Eq. (11) and Eqs. (24), (27), it is easy to find that

$$s = 1 + w_q - \frac{w'_q}{3w_q} + \frac{Q_1}{3\Omega_q}. \quad (28)$$

If $Q = 0$, Eqs. (27) and (28) reduce to Eqs. (13) and (14). It is worth noting that the forms of r and s in Eqs. (27) and (28) are derived only by using the general Friedmann equation, Raychaudhuri equation, and Eqs. (16) and (17) with a general interaction Q , and do not depend on any particular dark energy model. Therefore, the forms of r and s in Eqs. (27) and (28) can be used in *any* interacting dark energy model, while the subscript “ q ” is changed to the corresponding “ de ”. In fact, one can check that the r and s in e.g. [12, 15] are the special cases of our Eqs. (27) and (28) in particular cosmological models with particular forms of interaction Q .

In our interacting agegraphic dark energy model, to calculate the statefinder, we also need the w'_q in Eqs. (27) and (28). From Eqs. (22) and (20), we have

$$w'_q = \frac{\sqrt{\Omega_q}}{3n} \left[(1 - \Omega_q) \left(3 - \frac{2}{n} \sqrt{\Omega_q} \right) - Q_1 \right] - Q'_2. \quad (29)$$

If the interaction Q is specified, we can solve Eq. (20) to obtain $\Omega_q(z)$. Then, we get the statefinder $\{r, s\}$. In fact, there are many different forms of interaction Q in the literature (see e.g. [34, 35, 36, 37, 38] and references therein). For convenience, here we only consider a particular interaction form $Q = 3\alpha H \rho_q$, where α is a dimensionless constant. Therefore, in this case,

$$Q_1 = 3\alpha\Omega_q, \quad Q_2 = \alpha, \quad Q'_2 = 0. \quad (30)$$

In principle, α can be positive or negative. However, as pointed out in [8], the cases with positive α have physically richer phenomena. Thus, in this work, we only consider the cases with $\alpha \geq 0$. In Fig. 3, we show the evolution trajectories of the statefinder in the $r - s$ plane for different model parameters n and α in the interacting agegraphic dark energy model. While the universe expands, the trajectories of the statefinder start from the point $\{r = 1, s = 0\}$ when $a \rightarrow 0$, then s increases to a maximum and r decreases to a minimum, after that the trajectories turn a corner and approach another final fixed points when $a \rightarrow \infty$. From Eqs. (27)–(30), it is easy to find that $r \rightarrow 1$ and $s \rightarrow 0$ while $\Omega_q \rightarrow 0$ when $a \rightarrow 0$, whereas $r \rightarrow 1 + 2/n^2 - 3(1 + \alpha)/n$ and $s \rightarrow 2/(3n)$ while $\Omega_q \rightarrow 1$ when $a \rightarrow \infty$. From Fig. 3, we see that both n and α significantly affect the evolution trajectories of the statefinder in the $r - s$ plane. In addition, the present values of the statefinder for the interacting agegraphic dark energy model are fairly far from the one for the Λ CDM model, unless n is very large. Therefore, the statefinder diagnostic combined with the future SNAP observation can easily discriminate the interacting agegraphic dark energy model from the Λ CDM model.

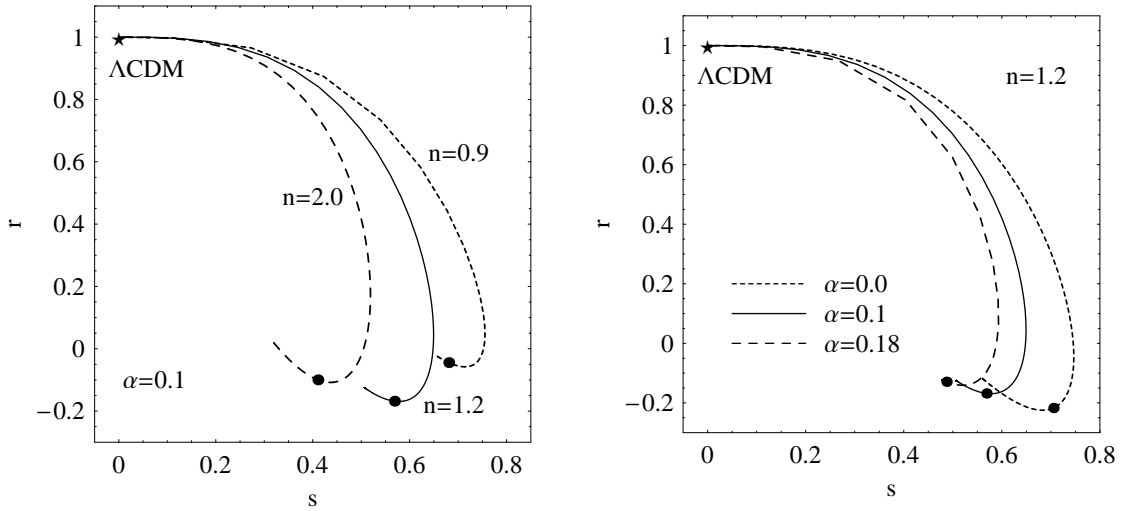


Figure 3: Evolution trajectories of the statefinder in the $r-s$ plane for different model parameters n and α in the interacting agegraphic dark energy model. The solid points indicate the present values of the statefinder. The statefinder for the Λ CDM model is a fixed point and is also indicated by a star symbol.

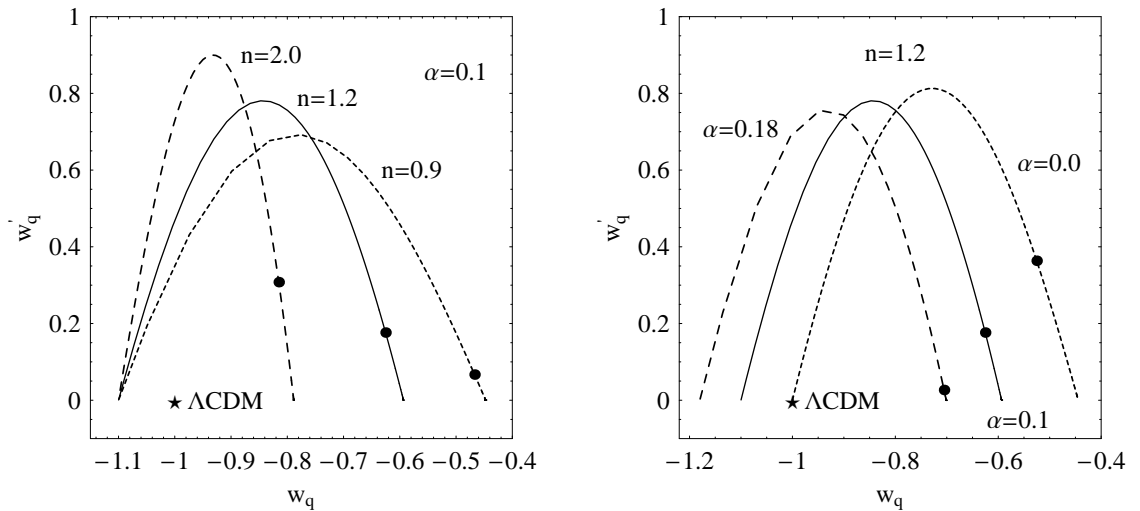


Figure 4: Evolution trajectories of $\{w_q, w'_q\}$ for different model parameters n and α in the interacting agegraphic dark energy model. The solid points indicate the present values of $\{w_q, w'_q\}$. The $\{w, w'\}$ of the Λ CDM model is a fixed point and is also indicated by a star symbol.

Using Eqs. (22) and (29), it is easy to obtain the evolution trajectories of $\{w_q, w'_q\}$ for different model parameters n and α in the interacting agegraphic dark energy model. We present the results in Fig. 4. While the universe expands, the trajectories start from a fixed point when $a \rightarrow 0$, then w'_q increases to a maximum, after that the trajectories turn a corner and approach another final fixed points when $a \rightarrow \infty$. From Eqs. (22) and (29), it is easy to find that $w_q \rightarrow -1 - \alpha$ and $w'_q \rightarrow 0$ while $\Omega_q \rightarrow 0$ when $a \rightarrow 0$, whereas $w_q \rightarrow -1 - \alpha + 2/(3n)$ and $w'_q \rightarrow 0$ while $\Omega_q \rightarrow 1$ when $a \rightarrow \infty$. Again, from Fig. 4, we see that both n and α significantly affect the evolution trajectories of $\{w_q, w'_q\}$ in the $w_q - w'_q$ plane. The most important observation from Fig. 4 is that w_q crossed the phantom divide $w = -1$ for the cases with $\alpha \neq 0$, which is impossible in the agegraphic dark energy model without interaction [8] (cf. Fig. 2). The interaction significantly changes the situation.

In summary, we investigated the agegraphic dark energy models without and with interaction by means of statefinder diagnostic and $w - w'$ analysis in this work. Both the statefinder $\{r, s\}$ and the $\{w_q, w'_q\}$ can be extracted from some future astronomical observations, especially the SNAP-type experiments [10, 23]. Therefore, they can be used to discriminate different cosmological models. In this work, our results suggest that the future SNAP observation can easily discriminate the agegraphic dark energy model from the Λ CDM model. In addition, since both the model parameters n and α significantly affect the evolution trajectories in the $r - s$ and $w_q - w'_q$ planes, the future astronomical observations can also discriminate the agegraphic dark energy models with different parameters.

After all, we admit that although the statefinder diagnostic and $w - w'$ analysis are commonly believed to be useful tools to discriminate different cosmological models [10, 23, 24], there are still some different attitudes (see [42] for instance). We hope that the future cosmological observations which are more precise can shed new light on this issue.

Acknowledgments

We are grateful to Prof. Shuang Nan Zhang for helpful discussions. We also thank Hui Li, Yi Zhang, Xing Wu, Bin Hu, Xin Zhang and Jingfei Zhang for useful discussions. This work was supported in part by a grant from China Postdoctoral Science Foundation, a grant from Chinese Academy of Sciences (No. KJCX3-SYW-N2), and by NSFC under grants No. 10325525, No. 10525060 and No. 90403029.

References

- [1] F. Károlyházy, *Nuovo Cim. A* **42**, 390 (1966);
F. Károlyházy, A. Frenkel and B. Lukács, in *Physics as Natural Philosophy*, edited by A. Simony and H. Feschbach, MIT Press, Cambridge, MA (1982);
F. Károlyházy, A. Frenkel and B. Lukács, in *Quantum Concepts in Space and Time*, edited by R. Penrose and C. J. Isham, Clarendon Press, Oxford (1986).
- [2] M. Maziashvili, gr-qc/0612110.
- [3] M. Maziashvili, arXiv:0705.0924 [gr-qc].
- [4] R. G. Cai, arXiv:0707.4049 [hep-th].

- [5] M. Li, Phys. Lett. B **603**, 1 (2004) [hep-th/0403127].
- [6] H. Wei and S. N. Zhang, arXiv:0707.2129 [astro-ph].
- [7] X. Zhang and F. Q. Wu, Phys. Rev. D **76**, 023502 (2007) [astro-ph/0701405].
- [8] H. Wei and R. G. Cai, arXiv:0707.4052 [hep-th].
- [9] V. Sahni, T. D. Saini, A. A. Starobinsky and U. Alam, JETP Lett. **77**, 201 (2003) [astro-ph/0201498].
- [10] U. Alam, V. Sahni, T. D. Saini and A. A. Starobinsky, Mon. Not. Roy. Astron. Soc. **344**, 1057 (2003) [astro-ph/0303009].
- [11] V. Gorini, A. Kamenshchik and U. Moschella, Phys. Rev. D **67**, 063509 (2003) [astro-ph/0209395].
- [12] W. Zimdahl and D. Pavon, Gen. Rel. Grav. **36**, 1483 (2004) [gr-qc/0311067].
- [13] X. Zhang, Phys. Lett. B **611**, 1 (2005) [astro-ph/0503075].
- [14] X. Zhang, Int. J. Mod. Phys. D **14**, 1597 (2005) [astro-ph/0504586].
- [15] J. Zhang, X. Zhang and H. Liu, arXiv:0705.4145 [astro-ph].
- [16] M. R. Setare, J. Zhang and X. Zhang, JCAP **0703**, 007 (2007) [gr-qc/0611084].
- [17] P. X. Wu and H. W. Yu, Int. J. Mod. Phys. D **14**, 1873 (2005) [gr-qc/0509036].
- [18] B. R. Chang, H. Y. Liu, L. X. Xu, C. W. Zhang and Y. L. Ping, JCAP **0701**, 016 (2007) [astro-ph/0612616].
- [19] B. Chang, H. Liu, L. Xu and C. Zhang, arXiv:0704.3670 [astro-ph].
- [20] Z. L. Yi and T. J. Zhang, Phys. Rev. D **75**, 083515 (2007) [astro-ph/0703630].
- [21] M. G. Hu and X. H. Meng, Phys. Lett. B **635**, 186 (2006) [astro-ph/0511615].
- [22] Y. Shao and Y. Gui, gr-qc/0703111.
- [23] E. E. O. Ishida, Braz. J. Phys. **35**, 1172 (2005) [astro-ph/0609614].
- [24] R. R. Caldwell and E. V. Linder, Phys. Rev. Lett. **95**, 141301 (2005) [astro-ph/0505494];
E. V. Linder, Phys. Rev. D **73**, 063010 (2006) [astro-ph/0601052].
- [25] R. J. Scherrer, Phys. Rev. D **73**, 043502 (2006) [astro-ph/0509890].
- [26] T. Chiba, Phys. Rev. D **73**, 063501 (2006) [astro-ph/0510598].
- [27] V. Barger, E. Guarnaccia and D. Marfatia, Phys. Lett. B **635**, 61 (2006) [hep-ph/0512320].
- [28] W. Zhao, Phys. Rev. D **73**, 123509 (2006) [astro-ph/0604460];
W. Zhao, arXiv:0706.2211 [astro-ph].
- [29] G. Calcagni and A. R. Liddle, Phys. Rev. D **74**, 043528 (2006) [astro-ph/0606003].
- [30] Z. K. Guo, Y. S. Piao, X. M. Zhang and Y. Z. Zhang, Phys. Rev. D **74**, 127304 (2006) [astro-ph/0608165].

- [31] Z. G. Huang, H. Q. Lu and W. Fang, hep-th/0610018;
Z. G. Huang, X. H. Li and Q. Q. Sun, *Astrophys. Space Sci.* **310**, 53 (2007) [hep-th/0610019].
- [32] R. de Putter and E. V. Linder, arXiv:0705.0400 [astro-ph].
- [33] E. V. Linder, arXiv:0704.2064 [astro-ph].
- [34] H. Wei and R. G. Cai, *Phys. Rev. D* **71**, 043504 (2005) [hep-th/0412045];
H. Wei and R. G. Cai, *Phys. Rev. D* **72**, 123507 (2005) [astro-ph/0509328];
H. Wei and R. G. Cai, *Phys. Rev. D* **73**, 083002 (2006) [astro-ph/0603052];
H. Wei and R. G. Cai, astro-ph/0607064;
H. Wei and S. N. Zhang, *Phys. Lett. B* **644**, 7 (2007) [astro-ph/0609597];
H. Wei and S. N. Zhang, arXiv:0704.3330 [astro-ph];
R. G. Cai and A. Wang, *JCAP* **0503**, 002 (2005) [hep-th/0411025].
- [35] Z. K. Guo, R. G. Cai and Y. Z. Zhang, *JCAP* **0505**, 002 (2005) [astro-ph/0412624];
Z. K. Guo and Y. Z. Zhang, *Phys. Rev. D* **71**, 023501 (2005) [astro-ph/0411524].
- [36] L. Amendola, *Phys. Rev. D* **60**, 043501 (1999) [astro-ph/9904120];
L. Amendola, *Phys. Rev. D* **62**, 043511 (2000) [astro-ph/9908023];
L. Amendola and C. Quercellini, *Phys. Rev. D* **68**, 023514 (2003) [astro-ph/0303228];
L. Amendola and D. Tocchini-Valentini, *Phys. Rev. D* **64**, 043509 (2001) [astro-ph/0011243];
L. Amendola and D. Tocchini-Valentini, *Phys. Rev. D* **66**, 043528 (2002) [astro-ph/0111535];
L. Amendola, C. Quercellini, D. Tocchini-Valentini and A. Pasqui, *Astrophys. J.* **583**, L53 (2003) [astro-ph/0205097].
- [37] W. Zimdahl and D. Pavon, *Phys. Lett. B* **521**, 133 (2001) [astro-ph/0105479];
W. Zimdahl and D. Pavon, *Gen. Rel. Grav.* **35**, 413 (2003) [astro-ph/0210484];
L. P. Chimento, A. S. Jakubi, D. Pavon and W. Zimdahl, *Phys. Rev. D* **67**, 083513 (2003) [astro-ph/0303145].
- [38] B. Gumjudpai, T. Naskar, M. Sami and S. Tsujikawa, *JCAP* **0506**, 007 (2005) [hep-th/0502191];
L. Amendola, M. Quartin, S. Tsujikawa and I. Waga, *Phys. Rev. D* **74**, 023525 (2006) [astro-ph/0605488];
Z. K. Guo, N. Ohta and S. Tsujikawa, *Phys. Rev. D* **76**, 023508 (2007) [astro-ph/0702015].
- [39] N. Sasakura, *Prog. Theor. Phys.* **102**, 169 (1999) [hep-th/9903146].
- [40] Y. J. Ng and H. Van Dam, *Mod. Phys. Lett. A* **9**, 335 (1994);
Y. J. Ng and H. Van Dam, *Mod. Phys. Lett. A* **10**, 2801 (1995);
S. Lloyd and Y. J. Ng, *Sci. Am.* **291**, 52 (2004).
- [41] W. A. Christiansen, Y. J. Ng and H. van Dam, *Phys. Rev. Lett.* **96**, 051301 (2006) [gr-qc/0508121];
M. Arzano, T. W. Kephart and Y. J. Ng, *Phys. Lett. B* **649**, 243 (2007) [gr-qc/0605117];
Y. J. Ng, gr-qc/0703096.
- [42] C. Cattoen and M. Visser, gr-qc/0703122.